ELSEVIER

Journal of Pharmaceutical and Biomedical Analysis
15 (1996) 83–98

JOURNAL OF
PHARMACEUTICAL
AND BIOMEDICAL
ANALYSIS

An oxazine reagent for derivatization of carboxylic acid analytes suitable for liquid chromatographic detection using visible diode laser-induced fluorescence

Sadayappan V. Rahavendran, H. Thomas Karnes *

Medical College of Virginia, Department of Pharmacy and Pharmaceutics, Richmond, VA 23298-0533, USA

Received for review 8 August 1995; revised manuscript received 26 February 1996

Abstract

This study reports the use of Nile Blue, an oxazine dye, as a derivatization reagent that fluoresces in the far-red spectral region and is suitable for derivatization with carboxylic-acid-containing analytes. Model carboxylic acid analytes such as benzoic acid, acetic acid, phenylacetic acid and hexanoic acid have been reacted as acid chlorides to form Nile Blue derivatives. The synthesis product of the Nile Blue benzoic acid derivative was confirmed using electrospray-mass spectrometry, infrared spectrometry, ^{1}H and ^{13}C nuclear magnetic resonance, reversed phase liquid chromatography (RP-HPLC), normal phase-thin layer chromatography, and spectral characterization. The synthesized Nile Blue derivatives, separated from reaction by-products with RP-HPLC, all demonstrated an approximately 10-fold drop in molar absorptivity and relative quantum yield. In addition, a 40 nm increase in Stokes shift was observed. A portion of the fluorescence was regained through post-column ionization of the Nile Blue benzoic acid derivative at pH 12. A RP-HPLC limit of detection of 88.25 fmol on column has been reported with conventional fluorescence detection-post-column ionization of the Nile Blue benzoic acid derivative. A limit of detection of 1.99 fmol on column (3.98×10^{-11} M) has been demonstrated for the Nile Blue benzoic acid derivative with the use of a laboratory-constructed visible diode laser fluorescence detector.

Keywords: Derivatization; Diode laser; Far-red label; Fluorescence detection; Liquid chromatography

1. Introduction

High performance liquid chromatography (HPLC) in combination with visible diode laser-induced fluorescence detection (VDLIF) has been shown to produce superior sensitivity and selectivity for the measurement of analytes in biological matrices [1]. Selectivity is enhanced because biological matrices demonstrate minimal blank fluorescence in the far-red regions (> 620 nm) of the spectrum. Outputs of diode lasers are optimal in this wavelength region and analytical methods can be provided that are instrument- rather than matrix-limited. Problems associated with sample degradation are also reduced considerably at long

* Corresponding author.

PII S0731-7085(96)01819-5

wavelengths and the intensity of Raman scatter is reduced by a factor of λ^{-4} [2]. Diode lasers have several advantages over conventional gas discharge light sources and laser sources (e.g. argon ion, helium–cadmium) by virtue of their long lifetimes (> 80 000 h), low noise characteristics, minimal power consumption, compact size, low cost and excellent spectral characteristics [3]. Although HPLC–VDLIF is an attractive technique for measuring low concentrations of analytes, its applicability is limited because few analytes possess native fluorescence in the relevant regions of the spectrum. To extend its applicability, derivatization to produce fluorophores in the far-red region is necessary for measuring these analytes [4]. Reagents which possess appropriate functional groups and which possess both absorption and fluorescence characteristics in the far-red spectral region when derivatized must therefore be developed.

Sauda et al. [5] have used Indocyanine Green, a commercially available near-infrard cyanine label, in the indirect detection mode through an ion-pair interaction for the measurement of analytes in biological matrices using HPLC–DLIF [5]. Patonay and co-workers [6–10] reported the synthesis of a number of near-infrared cyanine dyes containing functional groups for derivatization to amine, sulfhydryl and hydroxyl analyte moieties. Mank et al. [11] reported the measurement of 2-mercaptobenzotriazole (MBT), a pesticide, in spiked urine and river water through precolumn derivatization with CY5.4a, a laboratory synthesized far-red cyanine label. The detection limit of labeled MBT in the HPLC–VDLIF system was reported to be 8.0×10^{-12} M through serial dilution of the reaction mixture prepared at a higher concentration. Imasaka et al. [12] first reported the potential use of thiazine, oxazine and rhodamine analogs as fluorescent reagents with reactive functionalities suitable for VDLIF. With the use of a bifunctional reagent employing water-soluble carbodiimide, a number of oxazine and thiazine analogues were shown to bind covalently to albumin with theoretical on-column detection limits calculated to be in the low picomolar range. Attomole detection of amino acids covalently linked to azure B, a thiazine analog, with electrophoretic separation has also been reported [13].

The aim of this study was to develop a fluorescent reagent for precolumn derivatization with carboxylic-acid-containing analytes which fluoresce at far-red wavelengths. The derivatives formed should be suitable for measurement using a laboratory-constructed visible diode laser detector. Potential labels have been reviewed in the literature [14]. This work reports the use of Nile Blue, an oxazine reagent, as a label for carboxylic acid analytes. Model carboxylic acid analytes have been reacted with Nile Blue and their fluorescence characteristics studied. The limits of detection of a model derivative using both a commercially available conventional fluorescence detector and a laobratory-constructed diode laser detector are also presented.

2. Experimental

2.1. Chemicals

Nile Blue perchlorate, Toluidine Blue, Azure A, Azure B, Acid Blue 25, Alkali Blue 6B, Basic Blue 47, phenyl acetyl chloride, hexanoyl chloride, potassium bromide crystals (FT-IR grade), deuterated chloroform ($CDCL_3$), and deuterated methanol (CD_3OD) were purchased from Aldrich (Milwaukee, WI). Acetyl chloride, benzoyl chloride and sodium hydroxide pellets were obtained from Sigma (St. Louis, MO). Triethylamine was purchased from Fluka (St. Louis, MO) and trifluoroacetic acid (HPLC grade) from Pierce (Rockford, IL). Acetonitrile and methylene chloride were of HPLC grade and obtained from Baxter, B&J brand (Muskegon, MI). 1-Heptane sulfonic acid sodium salt (1-hydrate), HPLC grade, was purchased from Eastman (Rochester, NY). Sodium phosphate salts were purchased from Mallinckrodt (Paris, KY) and glacial acetic acid from J.T. Baker (Phillipsburg, NJ). Deionized water was distilled in the laboratory with a Corning mega pure automatic purification system (Corning, USA).

2.2. Apparatus

2.2.1. Spectral characterization

Absorbance spectral measurements were performed using a Perkin-Elmer model lambda 2S spectrometer equipped with deuterium and tungsten lamps. The spectrometer was linked to a computer using a Perkin-Elmer PECSS software package (Perkin-Elmer Corporation, Rockville, MD). Fluorescence spectral measurements were obtained using a Perkin-Elmer model LS-50 scanning luminescence spectrometer equipped with a pulsed xenon excitation source and a red-sensitive photomultiplier tube (PMT) model R928.

2.2.2. Derivatization equipment

Derivatization reactions were performed using Wheaton model 986217 3.0 ml clear borosilicate glass V-vials equipped with Wheaton model 986277 Teflon-lined solid top caps and Wheaton model 903063 spin vane stirring bars (Wheaton, Millville, NJ). Reactions were performed with a Pierce model 18970 reacti-therm heating/stirring module. Samples were vortexed using a Thermolyne model M16715 mixer (Thermolyne Corporation, Dubuque, IA) and centrifuged using an International Centrifuge model UV (International Equipment Company, Needham, MA). A Meyer N-Evap Organomation analytical evaporator (Associates Inc, Northborough, MA), was used for drying down samples using nitrogen gas.

2.2.3. Thin layer chromatographic (TLC) system and conditions

Normal phase (NP) silica gel GHLF plates (10 cm × 20 cm; 250 μm particle size; Analtech Incorporated, Newark, DE) with a solvent system consisting of 80% methylene chloride and 20% acetonitrile were used for the separation of the derivative from the unlabeled reagent. Visual detection was performed with a Spectroline model ENF-280C light source equipped with both short wavelength (254 nm) and long wavelength (365 nm) ultraviolet spectral outputs (Spectronics Corporation, Westbury, NY). Spectral characterization of the derivative spot was performed using non-fluorescent NP-TLC plates.

2.2.4. Liquid chromatographic system and conditions

The chromatographic system consisted of a Shimadzu Model LC-6A pump (Shimadzu Instruments, Columbia, MD), a Shimadzu model SCL-6A systems controller, a Shimadzu model SIL-6A autoinjector (20 μl injection volume) or a Rheodyne model 7125 manual injector equipped with a 20 μl or 50 μl sample loop (Cotati, CA), a Vydac model 201TP, C_{18} reversed phase (RP)-HPLC column (150 mm × 4.6 mm i.d.; 5 μm particle size) and a Vydac model 201GCC guard column (20 mm × 4.6 mm i.d., 5 μm particle size) packed with Vydac model 201 TP packing (The Separations Group, Mojave, CA). A Burdick and Jackson high ligand density model OC5 octyl column (150 mm × 4.6 mm i.d.; 5 μm particle size; Baxter, Muskegon, MI) was also used for the separation of the Nile Blue derivative from the unlabeled Nile Blue. Absorbance detection for determination and optimization of conjugate formation was performed using an ISCO model V^4 HPLC detector (Lincoln, NE) operating at a wavelength of 633 nm and equipped with both deuterium and tungsten lamps. Conventional fluorescence detection was performed using a Waters model 474 (Millipore Corporation, Milford, MA) detector equipped with a xenon lamp and a Hamamatsu model R928 red-sensitive PMT (Bridgewater, NJ). Data were recorded on a Hewlett Packard integrator model 3393A or 3396A (San Fernando, CA). The mobile phase consisted of acetonitrile–water–trifluoracetic acid (40:59.9:0.1, v/v/v) at a flow rate of 2.0 ml min^{-1}.

2.2.5. Electrospray ionization mass spectral analysis (ESI-MS)

ESI-MS was performed using an Extrel 4000 quadrupole mass spectrometer. Samples were introduced into the ESI source at 2.0 μl min^{-1} using a syringe pump. A voltage of 4.5 kV was maintained on the syringe needle to effect protonation of the sample. The spectrometer was scanned between 0 and 1050 m/z for a period of 5.19 min.

2.2.6. Infrared (IR) and nuclear magnetic resonance spectral analyses (^1H and ^{13}C NMR)

IR spectra were recorded with a Nicolet model 5ZDX FT-IR spectrometer using potassium bromide pellets. ^1H and ^{13}C NMR spectra were recorded on a Varian Gemini 300 spectrometer (Palo Alto, CA) at 300 MHz using $CDCl_3$.

2.2.7 Post-column ionization

The chromatographic system for post-column ionization of the Nile Blue derivative included a Shimadzu model LC-6A pump which was adjusted to deliver mobile phase (40% acetonitrile/59.9% water/0.1% trifluoroacetic acid) at a flow rate of 2.0 ml min^{-1} for the separation of the Nile Blue derivative from unlabeled Nile Blue. A Rheodyne model 7125 manual injector equipped with a 50 μl sample loop was used to inject samples onto a Vydac model 201GCC guard column and a Vydac model 201TP, C_{18} RP-HPLC column. The eluent from the chromatographic column was connected to the inlet of a 25 μl flowthrough mixing tee. Sodium hydroxide (0.50 M) was delivered to the second inlet of the flowthrough mixing tee at 35 μl min^{-1} using a Gilson model 302 reciprocating pump equipped with a model 5SC small volume pump head (Gilson Medical Electronics, Middleton, WI). The outlet of the flowthrough mixing tee was connected to either a Waters model 474 fluorescence detector or a laboratory-constructed visible diode laser detector. Data were acquired using a Hewlett Packard integrator model 3396A.

2.2.8. Visible diode laser detection

2.2.8.1. Instrumental design. The VDLIF detector (Fig. 1) consisted of a visible solid-state diode laser, Sanyo model SDL-3038 (Melles Griot, Boulder, CO), housed in an ILX-Lightwave model 4412 laser diode mount (ILX-Lightwave, Bozeman, MT) equipped with an ILX-Lightwave model 4014 collimating lens (5.0 mm focal length, 0.5 NA). The diode laser was tuned to 635 nm (output power 4 mW) with an ILX-Lightwave model LDC 3722 laser diode controller equipped with a current source and thermoelectric cooling unit (36 mA; 0.0°C). A stream of dry nitrogen was flowed continuously through the diode laser housing to prevent moisture formation on the output face of the diode laser. The output beam of the diode laser was focused onto a Hellma model 176.753 QS, 8 μl rectangular quartz flow cell (Hellma Cells, Jamaica, NY) housed in a cuvette holder (American Instrument Company, Silver Spring, MD). Fluorescence from the flow cell was collected at a 90° angle through an Oriel model 39311 fused silica biconvex lens (NA 0.63, Oriel Corporation, Stratford, CT), passed through two filters placed in series—a Corion model LL650 long pass filter ($\lambda_c = 650 \pm 5$ nm, transmittance = 80%; Corion Corporation, Holliston, MA) and a Melles Griot model 03FIV 024 band pass filter ($\lambda = 700$ nm, FWHM = 10 ± 2 nm, peak transmittance 50%; Melles Griot, Boulder, CO)—and onto a side-on Hamamatsu model R 928 red-sensitive PMT (Hamamatsu Corporation, Bridgeport, NJ). The PMT was placed in an Oriel model 70680 side-on housing. The lens and filters were attached to the PMT housing through Oriel models 7123 and 6213 flange-mounted cells. The PMT was adjusted to 1150 V with an Oriel Model 70705 high voltage power supply and the signal was collected using either a Keithley model 485 autoranging picoammeter (Keithley Instruments

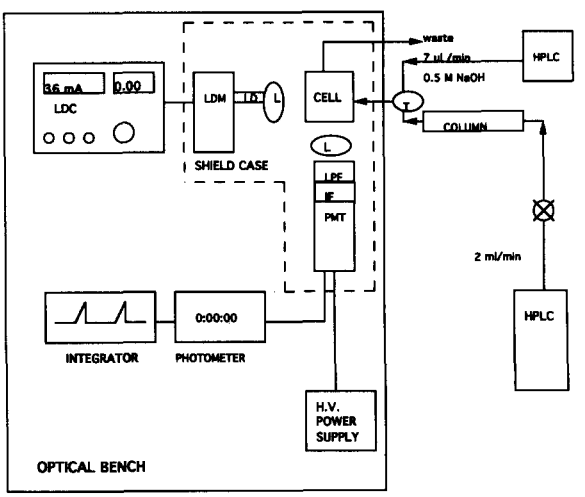

Fig. 1. Schematic of visible diode laser fluorescence detector: LDC, laser diode controller; LDM, laser diode mount; LD, laser diode, L, collimating lens; T, mixing tee; LPF, long pass filter; IF, bandpass filter; PMT, photomultiplier tube.

Inc., Cleveland, OH) or an Aminco model J10-281 digital photometer set to a 5 s time constant (American Instrument Company). Data were recorded onto a Hewlett Packard model 3396 A integrator. The diode laser mount, optics and PMT were mounted on an Oriel model 10988 honeycomb optical base plate (36 in. × 48 in.) to reduce noise due to vibrational shock. The diode laser mount was additionally protected from vibrational shock by mounting it on an Oriel model 11190 low profiled optical rail (1 m length) via an Oriel model 11641 carrier. The PMT was bolted to the optical base plate with an Oriel model 12153 magnetic base. The cuvette holder was held with a Fisher Scientific model 05-769-1 castaloy fixed angle clamp (Fisher Scientific, Pittsburgh, PA) which was then connected to two Oriel model 16021 precision translators placed one on top of the other (to provide accurate movement of the flow cell in both the *X* and *Y* directions) via an Oriel model 12320 rod and Oriel model 14421 rod holder. The precision translator was bolted to the honeycomb base plate. The optical portion of the instrument was shielded from ambient light with a black felt cloth held aloft by rods mounted on the honeycomb base plate.

2.2.8.2. Diode laser wavelength and power output. The output wavelength and power of the diode laser were measured with the use of an ILX-Lightwave model OMH-6720B silicon power/wavehead coupled to an ILX-Lightwave model OMM-6810B optical multimeter (ILX-Lightwave).

2.3. Methods

2.3.1. Choice of far-red label

2.3.1.1. Literature evaluation. Over 300 compounds used as dyes in textiles, stains in cell microscopy and as dyes in dye laser systems have been screened from the literature. Potential labels were chosen based on the presence of a derivatizable functional group, absorption in the far-red spectral region and prediction of fluorescence properties based on their structures (Fig. 2) [14,15].

2.3.1.2. Spectral analysis. Excitation and fluorescence spectra of the potential labels were acquired using the Perkin-Elmer luminescence spectrometer. Excitation spectra were scanned between 200 nm and 800 mn with the emission monochromator set to zero. Emission spectra were collected after setting the excitation monochromator to maximum. A 1.0 cm × 4.5 cm × 1.0 cm rectangular quartz cell was used for the fluorescence measurements. The relative quantum yield of the labels has been determined in 100% acetonitrile using the following equation [16]:

$$\phi_{label} = (AUC)_{fluorescence}/(AUC)_{excitation}$$

where ϕ_{label} = relative quantum yield of the label, $(AUC)_{fluorescence}$ = area under the fluorescence spectrum of the label, and $(AUC)_{excitation}$ = area under the excitation spectum of the label.

The relative quantum yields of the Nile Blue derivatives were also calculated by including the fluorescence characteristics of Nile Blue in the equation [17]. The area under the curve for each spectrum was calculated using the fluorescence data manager software program (FLDM) equipped for the Perkin-Elmer spectrometer.

Molar absorptivities of the labels prepared in 100% acetonitrile were calculated using the Beer–Lambert equation [18]. Molar absoptivities of the labels were calculated from the slopes of absorbance vs. concentration plots (a minimum of four concentration data points were used). Molar absorptivities were evaluated at the maximum absorption wavelengths of the labels. Dye concentrations in acetonitrile varied between 1×10^{-4} M and 1×10^{-7} M for relative quantum yield and molar absorptivity calculations.

2.3.2. Nile blue reagent for quantitiation of carboxyl-containing analytes

Derivatization of a carboxylic acid with a primary-amine-containing reagent (1-naphthylamine) in non-polar solvents has been previously reported by Ikeda et al. [19,20] who used a two-step process. The carboxylic acid was initially activated with thionyl chloride to produce the acid chloride. The primary amine reagent was then reacted with the acid chloride in the presence of a base catalyst to form the amide derivative. The reaction scheme used to form the Nile Blue derivatives is shown in Fig. 3.

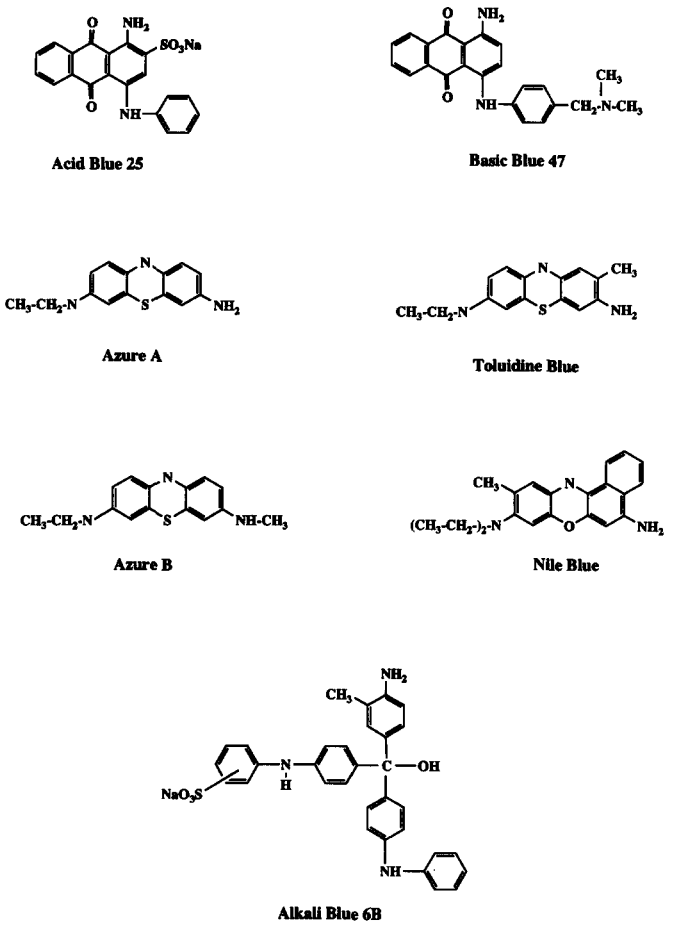

Fig. 2. Structures of selected farred labels.

2.3.3. Preparation of derivatization reagent

Nile Blue was purchased as a perchlorate salt and was found to be sparingly soluble in non-polar solvents. The derivatization procedure has typically been performed in non-polar solvents to provide a higher yield of the acid chloride [19]. 1-Heptane sulphonic acid was used as an ion-pair reagent for Nile Blue in this work, to effect phase transfer of Nile Blue from the aqueous layer to the organic layer. A 1.0 μmol ml^{-1} stock solution of Nile Blue heptane sulphonic acid was prepared by weighing 4.20 mg (10.0 μmoles) of Nile Blue perchlorate into a test tube and adding a 10-fold molar excess (23.0 mg) of 1-heptane sulphonic acid sodium acid sodium salt (1-hydrate). To the test tube 1.0 ml water and 2.0 ml methylene chloride were added. The solution was vortexed for 20 s and centrifuged at 2200 rev min^{-1} for 5.0 min to effect phase transfer of the Nile Blue sulphonic acid from the aqueous to the methylene chloride layer. The water layer was discarded; the methylene chloride layer was transferred into a 10.0 ml volumetric flask and diluted to volume with methylene chloride.

2.3.4. Derivatization reaction

Nile Blue sulphonic acid stock solution (250.0 μl) was pipetted into a V-vial and evaporated under a stream of dry nitrogen. The residue was reconstituted with 250 μl of acetonitrile. Triethylamine (5.0 μlmol), a base catalyst and 0.25 μ mol of the acid chloride in acetonitrile were added to the V-vial. A stirring vane was added to the V-vial, which was then capped and placed in the

reacti-therm heating/stirring module at 40°C for 20 min. The Nile Blue sulphonic acid prepared in methylene chloride was dried and reconstituted in acetonitrile because the derivatization reaction was performed at the boiling point of methylene chloride (40°C). Also, methylene chloride as a solvent was incompatible with the liquid chromatographic system. Nile Blue sulphonic acid was directly reacted with various acid chlorides (benzoyl chloride, acetyl chloride, phenylacetyl chloride and hexanoyl chloride) to avoid the initial activation step of the carboxylic acids to the acid chlorides with thionyl chloride.

2.3.5. Confirmation of the Nile Blue benzoic acid derivative

The formation of the Nile Blue–benzoic acid derivative was confirmed using NP-TLC, RP-HPLC and spectral characterization. Structural confirmation was obtained with ESI-MS, IR and NMR analyses.

2.3.5.1. NP–TLC. The reaction mixture (Nile Blue sulphonic acid + triethylamine + benzoyl chloride) and blank (Nile Blue sulphonic acid + triethylamine) were spotted (5.0 μl) in different lanes on the same plate. The developed plate was dried, the derivative spot (identified as a new spot distinguishable from the blank, i.e. based on R_f value) was scraped from the plate, dissolved in acetonitrile and centrifuged for 5 min to separate the derivative from the silica particles. The supernatant (derivative) was subjected to spectral characterization.

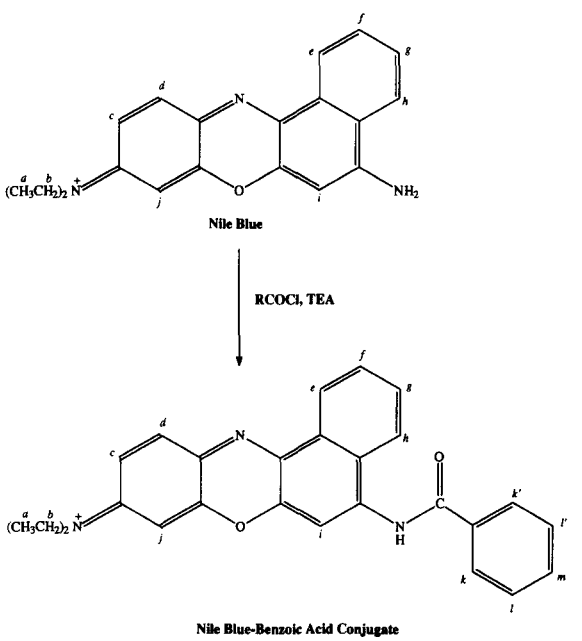

Fig. 3. Derivatization reaction scheme of acid chlorides with Nile Blue.

2.3.5.2. RP-HPLC. Multiple injections (50 μl) ($n = 3$) of the Nile Blue were made on the column to determine its retention time. The reaction mixture (50 μl) ($n = 3$) was also injected onto the column. The peak associated with unreacted Nile Blue in the reaction mixture was identified by spiking the reaction mixture with Nile Blue, and observing an increase in the area of the blank peak. The presence of the derivative peak was established by the formation of a peak at a longer retention time than the blank peak.

The concentration of derivative in the reaction mixture was determined by following the loss of the Nile Blue Peak chromatographically. This was performed independently by two methods. In the first method, equal concentrations of blank and reaction mixture were injected separately onto the column. The areas of the unreacted Nile Blue peaks in both the blank and reaction mixture were measured. The concentration of derivative formed in the reaction mixture was calculated as the product of the initial concentration of Nile Blue added to the reaction mixture and the fraction of derivaive formed. The fraction of the derivative formed was calculated by subtracting the peak area of unreacted Nile Blue in the reaction mixture from the peak area of the reagent (Nile Blue sulphonic acid + triethylamine). This result was then divided by the peak area of the reagent.

In the second method, a Nile Blue calibration curve (concentration vs. peak height response) was constructed by injecting triplicates at each concentration onto the column. The peak height of the unreacted Nile Blue in the reaction mixture was read off from the curve to obtain its concentration. The concentration of the derivative was calculated as the concentration of the unconverted Nile Blue in the reaction mixture subtracted from

the initial concentration of Nile Blue added to the reaction mixture.

2.3.5.3. Spectral characterization. The method of "peak trapping" was employed to collect the separated derivative, for further spectral evaluation. Trapping of the separated derivative was performed by determining the start and stop times for collection of the eluent (separated derivative peak) from when the peak tracing started and ended on the integrator. The time for collection was calculatd by dividing the volume of the eluent in the tubing connected to the exit of the flow cell by the flow rate of the eluent. The volume of eluent in the tubing was calculated by determining the volume of the tubing, which was $\pi r^2 h$. r^2 is the internal radius of the tubing; h is the length of tubing. The flow rate was calculated by measuring the volume of the mobile phase exiting the flow cell per minute.

The separated "peak-trapped" derivative concentraton was calculated by taking into consideration the dilution factor.

Excitation and emission spectra, molar absorptivity and relative quantum yield calculations of the derivative have been performed using the mobile phase as the solvent. The method has been explained previously (see Section 2.3.1.2.).

2.3.5.4. ESI-MS. ESI-MS data for the derivative were obtained by reacting an excess of benzoyl chloride relative to that of Nile Blue, thereby converting all the Nile Blue to the derivative. This was confirmed by injecting 50 μl of the reaction mixture onto the column. A peak relating to the retention time of unconverted Nile Blue was not detected. In addition, a 5 μl aliquot of the reaction mixture was spotted onto the NP-TLC plate and developed. A spot representing Nile Blue was absent. The reaction mixture was dried under a stream of dry nitrogen and reconstituted with 50% acetonitrile and 50% water prior to introduction into the ESI source.

2.3.5.5. IR and NMR. The derivative was synthesized in milligram quantities and was purified using NP column chromatography (silica gel 70–230 mesh, 60 Å, packed into a 20.0 cm × 2.0 cm glass column). A solvent composition of 100% ethylacetate was used to elute the derivative from the column. The derivative was dried under a stream of dry nitrogen and stored in a dessicator. NP-TLC development of the separated derivative showed the absence of spots corresponding to the R_f values for Nile Blue, benzoyl chloride and triethylamine. The derivative (1.0 mg) was prepared into a pellet using potassium bromide (100.0 mg) for IR analysis. Derivative concentrations of 5.0 mg ml^{-1} and 20.0 mg ml^{-1} were prepared in $CDCl_3$ for ^1H and ^{13}C NMR analyses respectively. Nile Blue was prepared in CD_3OD (5.0 mg ml^{-1}) and subjected to H NMR analysis.

2.3.6. Optimization of rection conditions for the formation of Nile Blue–benzoic acid derivative

The time of reaction for formation of the Nile Blue sulphonic acid–benzoic acid conjugate was studied in triplicate by reacting Nile Blue sulphonic acid, benzoyl chloride and triethylamine in a 1:1:20 molar ratio at 40°C. At time points 0, 10, 20, 30, 40, 50, 60, 80, 100 and 160 min, a 20.0 μl aliquout of the reaction mixture was transferred from the V-vial and reconstituted with 1.0 ml of mobile phase. A 20.0 μl aliquot was injected onto the column. The peak area of the conjugate was measured using absorbance detection at 633.0 nm.

Nile Blue sulphonic acid was reacted with benzoyl chloride nad triethylamine at 40°C for 10 min in duplicate at molar ratios 1:1:0, 1:1:1, 1:1:10, 1:1:100 and 1:1:1000, in order to study the effect of base (triethylamine) on the formation of the derivative. The samples were dried down under a stream of dry nitrogen and reconstituted with 1.0 ml of 100% acetonitrile. A 25.0 μl aliquot was transferred to a test tube and diluted with 500.0 μl of mobile phase. A 50.0 μl aliquot was then injected onto the column. The peak area of the conjugate was measured using absorbance detection at 633.0 nm.

2.3.7. Spectral characterization of the other Nile Blue derivatives

Acetyl chloride, phenylacetyl chloride and hexanoyl chloride were reacted with Nile Blue sulphonic acid. The derivatives were separated (RP-HPLC) and evaluated spectrally by the meth-

ods used for the Nile Blue–benzoic acid derivative.

2.3.8. Post-column ionization

2.3.8.1. Static system. The effect of pH on the fluorescence intensity of Nile Blue–benzoic acid was initially studied at extremes of pH (pH 2 and pH 13) by addition of triethylamine (50.0 μl) and trifluoroacetic acid (50.0 μl) separately to two test tubes each containing 4 ml of peak-trapped derivative. The pH of the two solutions was measured with a pHydrion Insta chek 0–13 pH paper (Microessential Laboratory, Brooklyn, NY). The excitation and fluorescence spectra as well as the intensity of the fluorescence were measured. The second step of the pH study was performed by spiking 1.0 ml of "peak-trapped" derivative to 4.0 ml of buffer solutions ranging from pH 3–pH13. The read mode of the fluorescence data manager was used. The excitation and emission monochromators (10.0 nm slit width) were set to 633.0 nm and 712.0 nm repsectively.

2.3.8.2. Preparation of buffer solutions. Buffer solutions were prepared using 0.005 M sodium phosphate monobasic (pH 5.37), 0.005 M sodium phosphate dibasic (pH 9.00) and 0.005 M sodium phosphate tribasic (pH 11.76). To obtain the appropriate pH, 4.0 N sodium hydroxide and glacial acetic acid were added. The final buffered derivative solution consisted of 1.0 ml of "peak-trapped" derivative added to 4.0 ml of the pH-controlled solution (50% acetonitrile/ 50% buffer).

2.3.8.3. Post-column ionization. A Gilson pump delivered 0.50 M sodium hydroxide to the mixing tee. Flow rates of 25, 30 and 35 μl min^{-1} were used to optimize the eluent from the mixing tee to a pH of 12. The pH of the eluent from the mixing tee was measured using pH paper (12–14) and a calibrated Corning model pH meter (Fisher Scientific, Pittsburg, PA).

2.3.9. Visible diode Laser detection

2.3.9.1. Instrumental design. Optimization of the diode laser beam size to pass through the flow cell without striking the walls of the cell was achieved by adjusting the distances between the collimated lens and the laser facet and the collimated lens and the flow cell. Fine tuning of the laser beam through the flow cell was performed by moving the flow cell in the X and Y directions using the precision translators. Spatial filtering of the fluorescence from the scatter was achieved by filling the flow cell with a solution of the reaction mixture and moving the PMT assembly back and forth to obtain the optimum analyte signal. The reaction mixture in the flow cell was flushed and replaced with mobile phase and the background signal due to scatter was recorded. This process of positioning the PMT assembly and measuring the analyte and background signals was repeated until the maximum analyte signal to background signal (optimal spatial filtering) was obtained.

Two bandpass filters and one long pass filter were used to selectively discriminate the fluorescence from the scattered radiation. Each filter was employed singly and then in combination. The most suitable arrangement was again determined from the maximum analyte signal to background signal.

A Keithley picoammeter and an Aminco photometer were evaluated individually for processing of anodic current from the PMT. A decision on the merits of each of the signal processors was based on the ability to electronically fllter out the noise component in the analyte signal. This process was performed by flrst injecting identical concentratons of the reaction mixture onto the column and then measuring the signal-to-noise obtained initially with the picoammeter and then with the photometer.

2.3.9.2. Diode laser wavelength and power output. The output beam of the diode laser was directed into the aperture of a silicon power/wavehead. The silcon power/wavehead was kept at a distance of 9.50 cm from the diode laser mount. The output wavelength of the diode laser was

Table 1
Spectral characteristics of selected far-red dyes

Dye	Purity[a] (%)	$\lambda_{ex};\lambda_{em}$ (nm)	Stokes shift (nm)	Σ (M^{-1} cm^{-1})	ϕ_f (%)
Nile Blue	98.0	633; 660	27	76 000	27.0
Azure A	70.0	630; 650	20	42 000	10.0
Azure B	95.0	638; 660	22	65 000	17.0
Toluidine Blue	90.0	631; 660	29	61 000	10.0
Basic Blue 47	45	617; 655	38	6 350	2.0
Acid Blue 25	45	624; 695	71	7 000	1.3
Alkali Blue 6B	50	631; 691	60	10 500	0.5

[a] As indicated by manufacturer.

monitored by varying the temperature to the diode laser. The maximum rated output power of 4.10 mW to prevent possible current-induced destruction of the semiconductor. A constant output of 4.10 mW was maintained by increasing the current to the diode laser with increasing temperature. The output wavelength of the diode laser was monitored by adjusting the temperature between 0°C and 25°C at 1°C intervals.

2.3.9.3. Limit of detection measurements. Limits of detection (LOD) for Nile Blue and its derivative were calculated as the concentration ($n = 3$) that provided a signal three times the mean peak-to-peak noise ($n = 3$) [21]. The peak-to-peak noise was determined by measurement of the noise in the baseline across the elution window of the intended peak.

3. Results and discussion

3.1. Choice of far-red label

Seven dyes were evaluated spectrally as potential labels for carboxyl-containing analytes and the results are summarized in Table 1. The labels were chosen from the oxazine, thiazine, anthraquinone and triphenylmethane classes of dyes. The spectral characteristics of the labels listed in Table 1 can be classified into two groups. The first group includes the oxazine and thiazine labels that possessed high molar absorptivities and narrow Stokes Shifts. The second class, the anthraquinone and triphenylmethane labels, possessed low molar absorptivities and broad Stokes shifts. These observations can be explained by the structural theory of luminescence spectroscopy [22]. Theory states that highly fluorescent compounds are planar, aromatic and highly conjugated. These structural factors are essential to effectively delocalize π electrons over the entire molecular structure (fluorescent ring system). This cloud of π electrons results in a compound exhibiting enhanced fluorescence characteristics. The small difference between the ground and excited molecular electronic energy levels (π–π^* transitions) in highely conjugated labels (e.g. oxazine and thiazine) results in the narrow Stokes shift observed. The anthraquinone and triphenylmethane labels are poorly conjugated molecules in contrast with the oxazine and thiazine labels. These compounds in contrast possess broad Stokes shifts (differences between ground and excited molecular electronic energy levels are large) and lower molar absorptivities (poorly conjugated). The poor fluorescence characteristics, in combination with the low commercial purity, of the anthraquinone and triphenylmethane dyes limit their use as precolumn reagents.

Nile Blue, and oxazine dye, was chosen as the far-red reagent because of its high molar absorptivity (75 000 M^{-1} cm^{-1}), high commercial purity ($> 98\%$), the presence of a reactive primary amine functionality, good solubility in commonly used RP-HPLC solvents and high photothermal stability. The excitation maximum of this reagent was also optimal for excitation by a diode laser oscil-

lating at 635.0 nm. Diode lasers emitting in the far-red region at room temperature are commercially available at wavelengths of 635.0 nm, 670.0 nm and 685.0 nm [23].

3.2. Nile Blue reagent for the quantitation of carboxyl-containing analytes

Carbodiimide, 2-chloro-1-methylpyridinium iodide (CMP), oxalyl chloride and thionyl chloride are some of the activiating reagents that have been used to derivatize a carboxylic acid analyte to an amine reagent [24]. In this study, thionyl chloride, carbodiimide and CMP were evaluated as activating agents. In optimization experiments, the Nile Blue reagent was directly reacted with the commercially available activated carboxylic acids to obviate this step.

3.2.1. Derivatization reaction

Ion pairing of Nile Blue with sulphonic acid was initially intended to make Nile Blue soluble in Methylene chloride for the derivatization reaction. Methylene chloride was not used as the derivatization solvent in this process but this practice was still followed becasue of effective removal of an impurity in the Nile Blue perchlorate salt. The impurity present in Nile Blue perchlorate has been identified as Nile Red [14]. An impurity peak eluting before the Nile Blue peak at a retention time of 2.8 min was observed when Nile Blue perchlorate was injected ($n = 3$) onto the RP-HPLC column. This peak was absent when Nile Blue sulphonic acid was injected ($n = 3$) onto the RP-HPLC column.

3.2.2. Confirmation of Nile Blue–benzoic acid derivative

3.2.2.1. NP-TLC. The R_f values for the Nile Blue and the derivative were 0.22 and 0.72. The measurement was repeated ($n = 3$) with plates from the same lot. The derivative was more non-polar than the label and therefore was less retained.

3.2.2.2. RP-HPLC. A resolution of >1.5 for the label and the derivative peaks was reproducibly observed ($n = 3$) with a mobile phase of acetonitrile:water:trifluoracetic acid (40:59.9:0.1, v/v/v) (Fig. 4). A nucleosil RP C_{18} column was used initially to separate the label. The label was eluted at $K' > 20$, which was impractical for routine use. The Vydac colum used in this work was not endcapped, and the enhanced selectivity of the analytes with the column may therefore be a result of secondary interactions.

The concentration calculated for the synthesized derivative was 99.0% with both methods. The assumptions used in both these cases was that loss of Nile Blue results in the formation of Nile Blue derivative. This observation was confirmed with NP-TLC. The reaction mixture on being developed showed the presence of only two main spots identified as the unreacted label and derivative.

3.2.2.3. Spectral characterization. Peak trapping of the separated derivative was performed by peak collection 5.0 s after the integrator traced the peak and 5.0 s after the peak tracing was completed. NP-TLC-and RP-HPLC-separated derivatives showed identical excitation and fluorescence spectra (Fig. 5). This confirmed spectrally that the

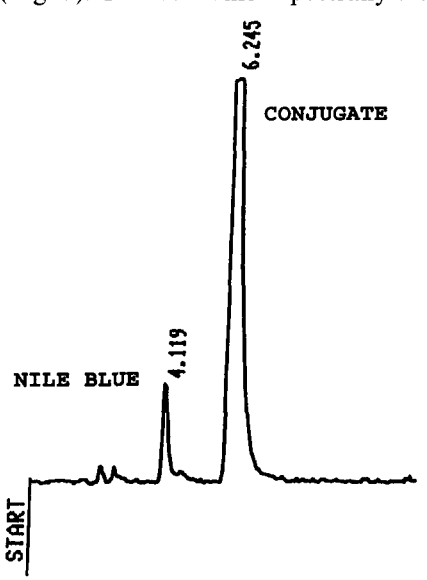

Fig. 4. Chromatogram of Nile Blue and Nile Blue–benzoic acid derivative.

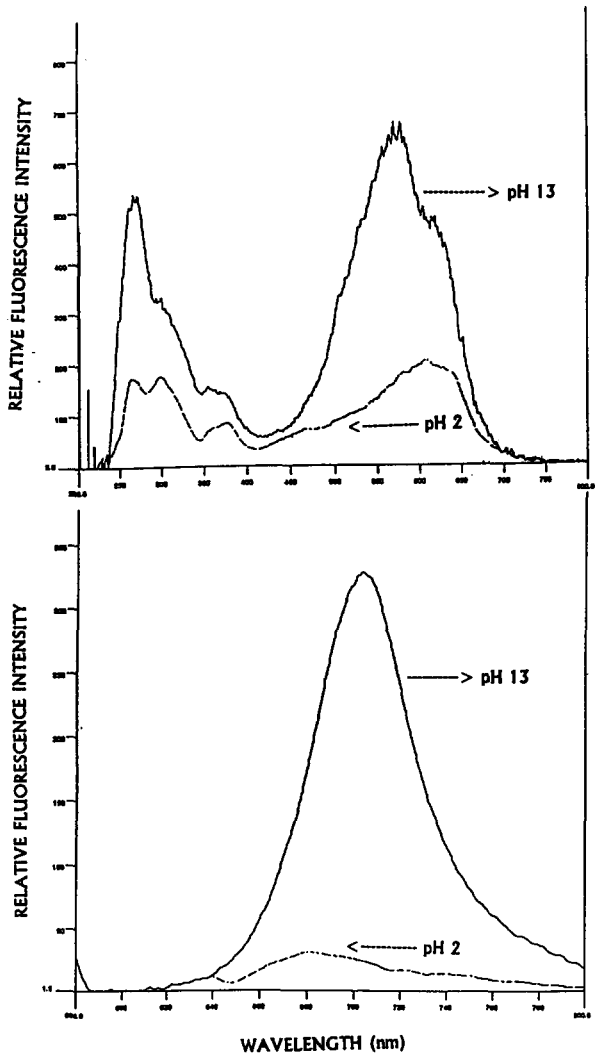

Fig. 5. (a) Excitation spectra of Nile Blue–benzoic acid derivative at pH 2 and pH 13; (b) emission spectra of Nile Blue–benzoic acid derivative at pH 2 and pH 13.

derivative separated by the two methods was the same product. The spectral characteristics of the labeled Nile Blue were significantly different from the unlabeled Nile Blue. The molar absorptivity and the relative quantum yield of the derivative were less by a factor of 10 than for the unlabeled Nile Blue. In addition there was an increase in the Stokes shift of the labeled Nile Blue (Table 2). This was attributed to a decrease in the extent of conjugation upon the formation of the amide derivative.

3.2.2.4. ESI-MS. The mass spectrum of the derivative demonstrated a molecular ion peak at 422 m/z units. The molecular weight of the Nile Blue sulphonic acid derivative was calculated to be 602 m/z units. The ESI system was set in the positive ion mode, so that the sulphonic acid m/z 179 peak would not appear in the mass spectrum. By subracting the mass of sulphonic acid from that of the derivative, a m/z value of 423 was obtained. The quadrupole was not operated at unit resolution and therefore a difference of one mass unit was insignificant.

3.2.2.5. IR and NMR. IR analysis of the derivative demonstrated peaks at 1315 cm^{-1}, 1589 cm^{-1}, and 1619 cm^{-1}. ^1H NMR (ppm) of Nile Blue in CD_3OD showed: δ 1.33 (6H, t, $J_{ab} = 7.11$ Hz, a), δ 3.69(4H, q, $H_{ba} = 7.10$ Hz, b), δ 6.83(1H, s, i), δ 6.91(1H, d, $J = 2.76$ Hz, aromatic H), δ 7.26(1H, dd, $J = 2.69$ Hz, $J = 6.78$ Hz, aromatic H) δ 7.83(2H, m, aromatic H's), δ 7.94(1H, t, $J = 8.21$ Hz, aromatic H), δ 8.29(1H, d, $J = 8.19$ Hz, aromatic H), δ 8.90(1H, d, $J = 8.22$ Hz, aromatic H). ^1H NMR (ppm) of the derivative in $CDCl_3$ showed: δ 1.23(6H, m, a), δ 3.42(4H, q, $J_{ab} = 7.10$ Hz, b), δ 6.32(1H, d, $J = 2.61$ Hz, aromatic H), δ 6.46(1H, s, i), δ 6.60(1H, dd, $J = 6.39$ Hz, $J, =$ 2.76, aromatic H), δ 7.5(4H, m, aromatic H's), δ 7.68(2H, m, aromatic H's), δ 8.12(2H, m, aromatic H's), δ 8.57(1H, d, $J = 7.74$ Hz, aromatic H), δ 8.52(1H, d, $J = 7.71$ Hz, aromatic H). The greatest downfield absorbance in ^{13}C NMR was observed at 158.44 ppm. The ^1H NMR spectrum for the derivative demonstrated five extra protons (k, k', l, l', m) compared to Nile Blue, providing verification of its structure (Figure 3). Both IR and ^{13}C NMR verified the presence of an amide linkage in the derivative.

3.2.3. Optimization of reaction conditions

The reaction for the synthesis of the derivative was complete after 10 min. This was established by measuring the peak areas at each time point. A reaction time of 20 min was therefore chosen as being optimal.

The effect of triethylamine on formation of the derivative in the range studied (molar ratios between 1 and 1000) demonstrated no increase in

Table 2
Spectral characteristics of Nile Blue and its derivatives

Analyte	λ_{ex}(nm)	λ_{em}(nm)	$\Sigma(M^{-1}\ cm^{-1})$	ϕ_f (%)
Nile Blue (NB)	633	660	76 000	27.00
NB–benzoic acid	633	699	12 000	2.40
NB–phenylacetic acid	631	690	18 000	3.10
NB–acetic acid	631	690	26 000	2.60
NB–hexanoic acid	638	680	20 000	2.90

the peak area of the derivative. When triethylamine was not added to the reaction mixture, the derivative was not detected. The acidic pH of the reaction mixture resulted in protonation of the amine functionality of the Nile Blue molecule, which prevented derivative formation. Triethylamine was added to the reaction mixture to prevent protonation of the amine functionality [24].

3.2.4. Spectral characterization of the other Nile Blue derivatives

The labeling of Nile Blue with benzoic acid resulted in the loss of a large portion of the fluorescence (Table 2). A rationale for loss of fluorescence is that the benzene ring of the benzoic acid molecule was electronegative and therefore attracted the lone pair of electrons on the nitrogen of the amide functionality. This would result in a decrease in the conjugation of the fluorescent ring system in the Nile Blue portion of the derivative. Nile Blue was reacted with structurally different acid chlorides: phenylacetyl chloride, acetyl chloride and hexanoyl chloride. Phenylacetyl chloride was chosen because the benzene ring was separated from the –NH–CO functionality by a $-CH_2$ group which may prevent attraction of electrons. Acetyl and hexanoyl chlorides are alkyl-type carboxylic acids and lack an electronegative group. The results in Table 2 demonstrate a similar loss of fluorescence across all the derivatives synthesized. The reasons for the loss of fluorescence can be attributed to the conversion of an electron-donating primary amine functionality to an electronegative (electron-withdrawing) amide functionality [25]. A similar explanation has been reported by Sens and Drexhage [26].

3.2.5. Post-column ionization

The effect of extremes of pH on the spectra of the Nile Blue–benzoic acid derivative is shown in Fig. 5. The fluorescence of the Nile Blue derivative at pH 12 was 11-fold higher than that of the derivative at pH 2. At pH 12 the excitation and emission maxima were centered at 580 nm and 712 nm respectively. The loss of fluoresence intensity by excitation of the derivative at 633 nm instead of at 580 nm was 1.5-fold and was negligible. The effect of pH on the fluorescence intensity of the derivative is shown in Fig 6. Maximum fluorescence was obtained at a pH of 12–13. A stability study was carried out at pH 12, 12.5 and 13. The fluorescence intensity of the derivative in these pH environments was recorded at time intervals of 10 min for a period of 60 min. The stability study wa carried out because of the observation that amides can hydrolyze at a basic pH [27]. The derivative at pH 13 exhibited a loss in fluorescence of approximately 35% after 60 min. This solution was injected onto the RP-HPLC column and demonstrated a loss in peak area, indicating hydrolysis of the derivative. The derivative at pH 12 exhibited no loss in fluorescence after 60 min. The post-column ionization results obtained from the static system were applied to the flowing system. The Gilson pump was set to a flow rate of 35 μl min^{-1} to provide a pH of 12 after mixing the eluent from the column.

3.2.5.1. Proposed mechanism for enhancement of fluorescence intensity. The portion of the derivative highlighted in a box (Fig. 3) resembles an imide functionality. The pK_a of an imide is typically between 8 and 10. At a pH of $\geqslant 12$ the nitrogen is unprotonated, resulting in a negative

charge. Fig. 6 shows the apparent pK_a of the derivative to be approximately 11.5. Therefore, following this rationale, one can predict that the nitrogen of the amine should be negatively charged. The negative charge on the nitrogen would then extend to conjugation of the fluorescent ring system to the Nile Blue portion of the molecule. This would result in enhancement of the fluorescence signal at pH $\geqslant$ 12. The mechanism presented is strengthened because unlabeled Nile Blue at pH 12 does no fluoresce at 712 nm.

3.2.6. Visible diode laser detection

3.2.6.1. Instrumental design. The optimal distance between the center of the flow cell and the collection lens was 4.50 cm. The combination of the long pass filter and the narrow band pass filter provided the best signal to peak-to-peak noise ratio by a factor of at least 1.70. Electronic filtering of the high frequency noise with the use of the Aminco photometer (time constant 5 s) improved the signal to peak-to-peak noise ratio by a factor of three with respect to the Keithley picoammeter.

3.2.6.2. Diode laser wavelength and power output. The diode laser wavelength was tuned between 635.0 nm and 640 nm over a temperature range between 0°C and 25°C. The diode laser was tuned to 635.0 nm with the temperature set to 0°C. A wavelength of 633.0 nm (maximum excitation of the derivative) can be theoretically obtained at lower temperatures, but maintaining constant temperature below 0°C over long periods of time was difficult to achieve with the present instrument. Addtional heat sinking would be necessary to run the diode laser at lower temperatures (to −20°C).

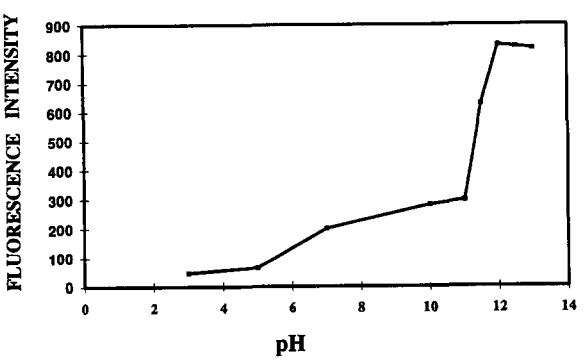

Fig. 6. Effect of pH on the fluorescence of the Nile Blue–benzoic acid derivative.

Table 3
On-column[a] detection limits (fmol) obtained for Nile Blue and its derivatives

Analyte	Conventional fluorescence	VDLIF
Nile Blue (NB)	11.21	0.246
NB–benzoic acid	960.00	88.50
NB–benzoic acid (PCl)	88.25	1.99

[a] 50 μl injection volume.

3.2.7. LOD

The LOD obtained with the conventional and VDLIF systems are summarized in Table 3. The results show that an approximately 10–40-fold enhancement in detection limits of the derivative has been obtained using post-column ionization. The relative quantum yield of the ionized derivative ($\phi = 12.0\%$) was five times higher than that of the unionized derivative ($\phi = 2.40\%$). The enhanced fluorescence characteristics of the ionized derivative resulted in a concentration LOD of 3.98×10^{-11} M using VDLIF detection. The LOD obtained in this work with an oxazine derivative is superior to that obtained by others [12]. The fluorescence of the derivative has been regained partially through post-column ionization and this is reflected by a lower LOD for Nile Blue (4.93×10^{-12} M). The LOD obtained using the VDLIF system was a factor of at least 10 better than the LOD of the conventional fluorescence system. Detection limits reported for laser-induced fluorescence systems have typically been between one and four orders of magnitude superior to those of conventional fluorescence systems [28]. The conventional fluorescence system used in this study is a factor of 50–1000 times more sensitive than the conventional detectors used by previous investigators to report comparisons with their laser detectors [29–31]. This enhanced sensitivity has been due to the advancement in electronic noise filtering devices and well designed

flow cells. The VDLIF system used in this study can be further optimized by utilizing a more efficient electronic noise filter to lower the present LOD by at least a factor of 5–10.

4. Conclusions

Nile Blue, an oxazine reagent, has been found to be suitable as a label for derivatization of carboxylic-acid-containing analytes. The use of this label had been suggested previously but had not been evaluated as presented in this work [12, 32]. The advantages of using this label as a derivatization reagent include its commercial purity, highly reactive functional group, cost, solubility in RP-HPLC solvents and ability to be excited with a suitable wavelength diode laser. The label loses a large portion of its fluorescence on derivatization but this has been shown to be partly regained through post-column ionization. The disadvantage of poor fluorescence of the derivative is offset by the presence of a large Stokes shift (approximately 100 nm with post-column ionization) which provides LOD that are comparable to that reported for a highly fluorescent far-red label [11]. The VDLIF instrument proved to be suitable for the detection of the derivatives. Further improvements in electronic filtering of the noise components are expected to increase the sensitivity of the system. Additionally, since diode lasers have been manufactured primarily for purposes other than spectrscopy [3], the output wavelengths of the diodes must be initially characterized prior to its use. Operating the diode laser at temperatures below 25°C improves the beam characteristics significantly [33]. Extensive research into the chemical engineering of far-red labels that provide highly fluorescence characteristics and large Stokes shifts on derivatization is required in order for this technique to develop further.

Acknowledgements:

The authors thank Mr. Hariharan Nair and Dr. V. Wysocki of the Department of Chemistry, VCU, for performing ESI-MS on the samples, the Department of Medicinal Chemistry, VCU, for the use of their IR and NMR spectrometers and Dr. Mike Crawford of ILX-Lightwave for the loan of the laser diode controller.

References

[1] S.V. Rahavendran and H.T. Karnes, Pharm. Res., 10 (1993) 328–334.
[2] C.M.B. Van Den Beld and H. Lingeman, in W.R.G. Baeyens, D.D. Kenkeleive and K. Korkidis (Eds.), Luminescence Techniques in Chemical and Biochemical Analysis, M. Dekker, New York, 1990, pp. 237–316.
[3] T. Imasaka and N. Ishibashi, Anal. Chem., 62 (1990) 363A–371A.
[4] J. Goto, in H. Lingeman and W.J.M. Underberg (Eds.), Detection Oriented Derivatization Techniques In Liquid Chromatography, M. Dekker, New York, 1990, pp. 323–330.
[5] K. Sauda, T. Imasaka and N. Ishibashi, Anal. Chem., 58 (1986) 2649–2653.
[6] J. Sena and G. Patonay, Anal. Chem., 63 (1991) 2934–2938.
[7] D.A. Willberforce and G. Patonay, Appl. Spectrosc., 43 (1989) 1450–1455.
[8] M.D. Antoine, S. Devanathan and G. Patonay, Spectrochim. Acta, Part A, 47 (1991) 501–508.
[9] A.E. Boyer, S. Devanathan, D. Hamilton and G. Patonay, Talanta, 39 (1992) 505–510.
[10] G. Patonay and M.D. Antoine, Anal. Chem., 63 (1991) 321A–327A.
[11] A.J.G. Mank, E.J. Molenaar, H. Lingeman, C. Gooijer, U.A.T. Brinkman and N.H. Velhorst, Anal. Chem., 65 (1993) 2197–2203.
[12] T. Imasaka, A. Tsukamoto and N. Ishibashi, Anal. Chem., 61 (1989) 2285–2288.
[13] T. Higashijima, T. Fuchigami, T. Imasaka and N. Ishibashi, Anal. Chem., 64 (1992) 711–714.
[14] F.J. Green, The Sigma–Aldrich Handbook Of Stains, Dyes and Indicators, Aldrich Chemical Company Inc., Milwaukee, WI, 1990.
[15] D.R. Waring and G. Hallas (Eds.), The Chemistry and Application of Dyes, Plenum Press, New York, 1990.
[16] J.D. Weinefordner, S.G. Schulman and T.C. O'Haver, Luminescence Spectrometry in Analytical Chemistry, Wiley-Interscience, New York, 1972.
[17] G.G. Guilbault, Practical Fluorescence: Theory, Methods and Techniques, Dekker, New York, 1973.
[18] H.H. Willard, L.L. Merrit, Jr., J.A. Dean and F.A. Settle, Jr., Instrumental Methods of Analysis, 7th edn., Wadsworth Publishing Compnay, Belmont, CA, 1988.
[19] M. Ikeda, K. Shimada and T. Sakaguchi, Chem. Pharm. Bull., 30 (1982) 2258–2261.
[20] M. Ikeda, K. Shimada and T. Sakaguchi, J. Chromatogr., 272 (1983) 251–259.

[21] Kenneth Ogan, in E. Katz (Ed.), Quantitative Analysis using Chromatographic Techniques, John Wiley & Sons, Chichester, UK, 1987, p.33.
[22] S.G. Schulman, Fluorescence and Phosphorescence Spectroscopy: Physicochemical Principles and Practice, Pergamon Press, Oxford, 1977.
[23] J. Hecht, Laser Focus World, 28 (1992) 127–143.
[24] H. Lingeman, A. Huslhoff, W.J.M. Underberg and F.B.J.M. Offerman, J. Chromatogr., 290 (1988) 215–222.
[25] K. Nakanishi and P.H. Solomon, Infrared Absorption Spectroscopy, 2nd edn., Holden–Day, Inc., San Franciso, CA, 1977.
[26] R. Sens and K.H. Drexhage, J. Lumin., 24 (1981) 709–712.
[27] T.L. Lemke, Review of Organic Functional Groups: Introduction to Medicinal Organic Chemistry, 2nd edn., Lea and Febiger, Philadelphia, PA, 1988.
[28] C.M.B. Van den Beld, H. Lingeman, G.J. Van Ringen, U.R. Tjaden and J. Van der Greef, Anal. Chim. Acta, 205 (1988) 15–27.
[29] M.C. Roach and M.D. Harmony, Anal. Chem., 59 (1987) 411–415.
[30] K. Sauda, T. Imasaka and N. Ishibashi, Anal. Chim. Acta, 187 (1986) 353–356.
[31] N.J. Dovichi, J.C. Martin, J.H. Jett and R.A. Keller, Science, 219 (1983) 845–847.
[32] T. Imasaka, T. Higashijima and N. Ishibashi, Anal. Chim. Acta, 251 (1991) 191–195.
[33] L. Hollberg, Appl. Laser. Spectrosc. Phys., 242 (1990) 117–125.